Biosensors and Bioelectronics 53 (2014) 363–369

Contents lists available at ScienceDirect

Biosensors and Bioelectronics

journal homepage: www.elsevier.com/locate/bios

Signal-on electrochemiluminescence of biofunctional CdTe quantum dots for biosensing of organophosphate pesticides

Han Liang, Dandan Song, Jingming Gong *

Key Laboratory of Pesticide & Chemical Biology of Ministry of Education, College of Chemistry, Central China Normal University, Wuhan 430079, PR China

ARTICLE INFO

Article history:
Received 7 September 2013
Received in revised form
7 October 2013
Accepted 7 October 2013
Available online 16 October 2013

Keywords:
Electrochemiluminescence
Acetylcholinesterase
Quantum dots
Organophosphate pesticides
Dissolved oxygen
Signal-on model

ABSTRACT

A new, highly sensitive and selective ECL assay biosensor based on target induced signal on has been developed for the detection of organophosphate pesticides (OPs), whereby the smart integration of graphene nanosheets (GNs), CdTe quantum dots (CdTe QDs), and acetylcholinesterase (AChE) enzymatic reaction yields a biofunctional AChE–GNs–QDs hybrid as cathodic ECL emitters for OPs sensing. The electrochemically synthesized GNs were selected as a supporting material to anchor CdTe QDs, exhibiting a significantly amplified ECL signal of QDs. On the basis of the effect of OPs on the ECL signal of AChE–QDs–GNs modified glassy carbon electrode (GCE), a highly sensitive GNs-anchored-QDs-based signal-on ECL biosensor was developed for sensing OPs, combined with the enzymatic reactions and the dissolved oxygen as coreactant. The conditions for OPs detection were optimized by using methyl parathion (MP) as a model OP compound. Under the optimized experimental conditions, such a newly designed system shows remarkably improved sensitivity and selectivity for the sensing of OPs. The detection limit was found to be as low as about 0.06 ng mL^{-1} ($S/N=3$). Toward the goal for practical applications, the resulting sensor was further evaluated by monitoring MP in spiked vegetable samples, showing fine applicability for the detection of MP in real samples.

1. Introduction

Organophosphates pesticides (OPs) exposure is a growing global health problem, posing a highly severe threat on human life (Arduini et al., 2006; Li et al., 2007). High level exposure to OPs results in the inhibition of acetylcholinesterase (AChE) activity, which may cause respiratory paralysis and death (Kim et al., 2005). Therefore, rapid determination and reliable quantification of trace level of OPs have become increasingly important. Well established methods over the past decades for OPs monitoring include various chromatographic techniques coupled with various detectors (Albanis et al., 2004; Rotiroti et al., 2005; Leandro et al., 2006). These methods, however, require complicated pretreatment steps, extensive labor resources, and are not applicable for on-site determination. Obviously, an effective analytical method for rapid screening of OPs residues is urgently needed.

Electrochemiluminescence (ECL) is chemiluminescence triggered by electrochemical methods (Richter, 2004; Miao, 2008). Owing to the advantages, such as good stability against photobleaching, simplified optical setup, low cost, and low background noise, ECL has widely been investigated as a facile, fast, sensitive, and cost-effective analytical technique (Dennany et al., 2003; Guo and Dong, 2004; Dai et al., 2009; Liu and Ju, 2008). In particular, since the first reported ECL of Si quantum dots (QDs) (Ding et al., 2002), the QDs-based ECL emission has become more and more attractive in the analytical fields, such as DNA analysis (Shan et al., 2009; Huang et al., 2010; Huang and Zhu, 2009; Zhang et al., 2008; Wang et al., 2008), immunoassays (Bertolino et al., 2005; Kurita et al., 2010; Liu et al., 2010, 2013; Liang et al., 2012a; Li et al., 2013; Li et al., 2011), cell assays (Han et al., 2010; Nie et al., 2013), detection of other biological molecules (biomarker analysis, catechol derivatives, thrombin, and cystein, etc) (Liu et al., 2007; Deng et al., 2011; Jie and Yuan, 2012), and metal ions (Qiu et al., 2011; Cheng et al., 2012). Recently, several comprehensive reviews about nanomaterials-based ECL (including QDs) have been successively published (Lei and Ju, 2011; Huang et al., 2011; Li et al., 2012; Rampazzo et al., 2012). As known, the ECL signals of pure QD are very weaker. To efficiently enhance the ECL emission, a critical issue is how to realize the amplification of ECL signal. In this regard, various QDs-based ECL signal transduction emitters with highly intense ECL, including QDs–carbon nanotubes (CNTs) (Wang et al., 2009a; Ding et al., 2006), QDs–graphene (Liu et al., 2013; Yang et al., 2013; Wang et al., 2009b, 2012; Huang et al., 2010; Deng et al., 2011, QDs–carbon nanospheres (Zhang et al., 2011) and magnetic Fe_3O_4–QDs composite (Jie and Yuan, 2012) have been developed for improving the sensitivity and the analytical performance of ECL sensors, especially in the detection of trace substance. Despite these outstanding achievements, these

* Corresponding author. Tel.: +86 27 6786 7535.
E-mail address: jmgong@mail.ccnu.edu.cn (J. Gong).

0956-5663/$ - see front matter © 2013 Elsevier B.V. All rights reserved.
http://dx.doi.org/10.1016/j.bios.2013.10.011

strategies are mainly based on the quenching or inhibition effect of the analyte on the QDs ECL, *i.e.* a signal-off ECL detection mode. As known, signal-on detection is preferred over signal-off detection due to the serious false positives aroused by interference in signal-off detection (Liao et al., 2013; Shen et al., 2012). To meet the fast-developing detection requirements (e.g. simple operations, high sensitivity, economical expense, and portable instruments), it is still a great challenge to exploit a high-performance ECL signal transduction emitters in a simple and facile approach for sensing applications.

Over the past few years, enzyme-based inhibition biosensors have emerged as a promising alternative for pesticides analysis (Gong et al., 2009; Li et al., 2007; Bachmann et al., 1999; Won et al., 2010; Chauhan and Pundir, 2012; Gong et al., 2013), where acetylcholinesterase (AChE) enzyme activity was employed as an indicator of quantitative measurement of insecticides. The product of the enzymatic reaction, thiocholine could react with the dissolved oxygen, a typical coreactant of QDs ECL. Upon the addition of OPs, the inhibition on AChE enzyme system would occur, and induce the consumed dissolved oxygen decrease, thus leading to the enhanced ECL signal, a signal-on ECL mode. Inspired by this, here we present for the first time, the novel applications of the electrochemically reduced GNs-anchored-QDs, combined with the enzymatic reactions, for signal-on ECL sensing of OPs.

Herein, the electrochemically reduced GNs were selected as a supporting material to anchor CdTe QDs. It has been proved that the electrochemical reduction of the exfoliated graphene oxide (GO) is a green and facile way to synthesize large-scale graphene film in high quality (Guo et al., 2009; Gong et al., 2012b). And moreover, GNs-anchored-QDs composite has shown the promising luminescence properties, exhibiting a significantly amplified ECL signal of QDs (Liu et al., 2013; Li et al., 2011; Deng et al., 2011; Wang et al., 2009b). The amplified ECL emission thus provides the feasibility for ECL analysis of trace pollutants. The smart integration of GNs, AChE enzyme, and CdTe QDs ECL yields a biofunctional AChE–GNs–CdTe QDs hybrid as cathodic ECL emitters for OPs sensing. Since the enzymatic reactions consume the dissolved oxygen (as coreactant of QDs ECL), upon the addition of OPs, the cathodic ECL signal of QDs would be greatly influenced due to AChE inhibition induced. On the basis of the effect of OPs on the ECL signal of CdTe QDs, a new rapid and sensitive QDs-based signal-on ECL approach was developed for OPs sensing. The mechanism of cathodic ECL of CdTe QDs on the AChE–QDs–GNs/GCE was shown in Scheme 1. To the best of our knowledge, this is the first report on utilizing biofunctional AChE–GNs–CdTe QDs sensing platform for OPs ECL analysis. Encouragingly, the combination of graphene, enzyme reaction, the dissolved oxygen as coreactant, and QDs-based ECL opens up new opportunities for fast, simple and sensitive analysis of OPs.

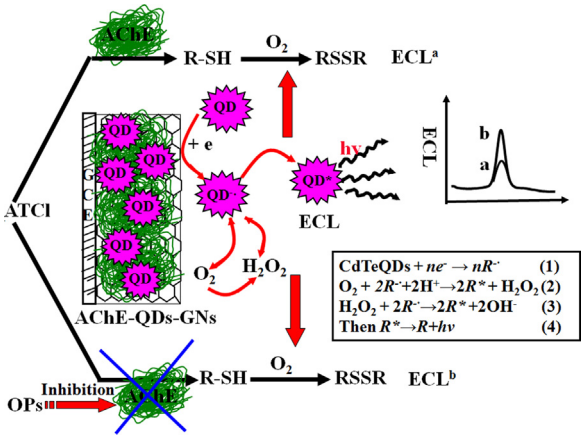

Scheme 1. Schematic illustration for the principle of signal-on ECL biosensor for the determination of OP compound using AChE–QDs–GNs/GCE.

2. Experimental

2.1. Reagents and apparatus

$CdCl_2 \cdot 2.5H_2O$ was obtained from Jinshan Tingxin Chemical Plant (Shanghai, China). $NaBH_4$ (96.0%) were obtained from Tianjin Chemical Reagent Plant (Tianjin, China). Thioglycolic acid (TGA) and Na_2TeO_3 were obtained from Sinopharm Chemical Reagent Co., Ltd. (American). Acetylthiocholine chloride (ATCl) and AChE (Type C3389, 500 U mg^{-1} from electric eel) were purchased from Sigma-Aldrich (St. Louis, USA) and used as received. Methyl parathion (MP) was obtained from Treechem Co. (Shanghai, China). All other chemicals were of analytical grade and used as received without further purification. Phosphate buffer solutions (PBS, 0.1 M) with various pH values were prepared by mixing stock standard solutions of K_2HPO_4 and KH_2PO_4. All aqueous solutions were prepared with doubly distilled water. All experiments were carried out at room temperature.

Photoluminescence (PL) spectra were acquired with a PerkinElmer Model LS-55 luminescence spectrometer. The ultraviolet–visible (UV–vis) absorption spectra were performed on a Thermo Nicolet Corporation Model evolution 300 spectrophotometer. The general morphology of the products was characterized by the scanning electron microscopy (SEM, JSM-5600). ECL studies were performed on a MPI-E multifunctional electrochemical and chemiluminescent analytical system (Xi'an, China). The voltage of the photo multiplier tube (PMT) was biased at 800 V during the whole processes. Electrochemical impedance spectroscopic (EIS) analysis was performed on CHI 660D electrochemical workstation (CHI, USA) in 5 mM $K_3Fe(CN)_6/K_4Fe(CN)_6$ with 0.1 M KCl as the supporting electrolyte. A conventional three-electrode system was used for the electrolytic system, a glassy carbon electrode used as the working electrode, a platinum wire as the counter electrode, and an Ag/AgCl (saturated KCl) electrode as the reference electrode.

2.2. Synthesis of thiol-capped CdTe QDs

The CdTe QDs capped with thiols were synthesized according to the literature (Li et al., 2010) with little modification. Briefly, 38 ml of ultrapure water and 10 ml of 0.01 M $CdCl_2$ were transferred to a small flask under N_2 atmosphere and held for about 15 min. Then, 10 μl of TGA was added quickly, followed by adjustment of the pH to 11.0 by dropwise addition of 1 M NaOH, until the mixture became clear. A 55.5 mg quantity of tri-sodium citrate and 2 ml of 0.01 M Na_2TeO_3 were injected into the above mixture solution. Finally, 3.0 mg of $NaBH_4$ was added, and the solution was deaerated by highly pure N_2 bubbling for 10 min. After mixing, about 25 ml of this mixture was transferred to a reaction kettle, heated to 180 °C and refluxed for 60 min; thus, thiol-capped CdTe QDs could be obtained. Afterward, the resulting products were precipitated by acetone, and superfluous TGA and Cd^{2+} were removed by centrifugation at 3000 rpm for 5 min. The resultant precipitate was redispersed in water, reprecipitated three times by a copious amount of acetone, and then kept in the dark for further use.

2.3. Preparation of GO and GNs

GO was synthesized from graphite by the modified Hummers method (Hummers and Offeman, 1958; Kovtyukhova et al., 1999). The as-synthesized graphite oxide was suspended in water and subjected to dialysis for one week to remove residual salts. After dried at 5 °C overnight, the as-purified graphite oxide was exfoliated into GO by ultrasonicating a 0.05 wt% aqueous dispersion for 30 min. Unexfoliated graphite oxide was removed by a 5 min

ultrafiltration at 2000 rpm. GNs were acquired by scanning the GO/GCE between 0 and −1.5 V for 10 cycles in pH 7.0 PBS.

2.4. Fabrication of ECL biosensors

Prior to modification, the basal GCE was polished to a mirror finish using 1.0, 0.3 and 0.05 μm alumina slurries. After each polishing, the electrode was sonicated in ethanol and doubly distilled water for 5 min, successively, in order to remove any adsorbed substances. Finally, it was dried under nitrogen atmosphere ready for use. Ten microlitres of 0.1 mg mL^{-1} GO dispersion was dropped onto the surface of the cleaned GCE and was kept at room temperature till dry (labeled as GO/GCE). To obtain electrochemically reduced GNs modified electrode, GO/GCE was scanned between 0 and −1.5 V for 10 cycles in pH 7.0 PBS. Then, 10 μL of a certain concentration of QDs solution was dropped onto GNs film and dried in air (labeled as QDs–GNs/GCE). QDs–GNs/GCE was further coated with 10 μL of AChE solution and dried at 4 °C. Finally, the enzymes were cross-linked by glutaraldehyde by vapor-bathing for 10 min to fabricate a stable AChE–QDs–GNs/GCE. The biosensor was stored in 0.1 M pH 7.0 PBS in 4 °C refrigerator when not in use.

2.5. Measurement procedure

For the measurements of MP, the obtained AChE–QDs–GNs/GCE was first immersed in PBS solution containing different concentrations of standard MP for 20 min, and then transferred to the solution of 1.0 mL pH 8.0 PBS containing 1.0 mM ATCl to study the electrochemical response by ECL. The concentration of 1.0 mM ATCl is an optimized value.

3. Results and discussion

3.1. Characterization of QDs, GNs, and AChE–QDs–GNs

The PL and UV–vis absorption spectra of the CdTe QDs are shown in Fig. 1A. The PL emission peak was at 720 nm and the maximum absorption wavelength was at 640 nm, indicating the consequence of quantum confinement. The size of the CdTe QDs, estimated from the empirical equations reported previously (Yu et al., 2003), was about 3.2 nm.

$$D = (9.8127 \times 10^{-7})\lambda^3 - (1.7147 \times 10^{-3})\lambda^2 + 1.0064\lambda - 194.84$$

In the above equation, λ (nm) is the wavelength of the first excitonic absorption peak of the UV–vis absorption spectrum. Inset of Fig. 1B illustrates the cyclic voltammetric responses for the formation processes of GNs on the GCE. The cyclic voltammograms of an exfoliated GO/GCE in a potential range from 0.0 to −1.5 V shows a large cathodic current peak at around −1.20 V vs. SCE with a starting potential of −0.75 V vs. SCE. This large reduction current should be due to the reduction of the surface oxygen groups. In subsequent cycles, the reduction current at negative potentials decreases considerably and disappears finally. This demonstrates that the reduction of surface-oxygenated species at GO occurs quickly and irreversibly, and the exfoliated GO could indeed be reduced electrochemically at negative potentials to form GNs/GCE, agreeing well with the previous report (Guo et al., 2009; Gong et al., 2012b). Typical SEM image of the as-synthesized GNs shows 2D nanosheet morphologies, exhibiting a few thin wrinkles onto the surface (shown in Fig. 1B). These nanosheets with slightly scrolled edges were closely associated with each other to form a disordered solid surface. With the further modification of AChE, the SEM image showed rough and open structure of AChE–QDs–GNs (Fig. 1D), which was obviously different from the morphology of QDs–GNs (Fig. 1C), and made the substrate easily access to the enzyme molecules.

The capability of electron transfer of different electrodes was investigated by electrochemical impedance spectra (EIS), shown in Fig. 2A. It can be seen that EIS of the bare GCE is composed of a semicircle and a straight line featuring a diffusion-limiting step of the $Fe(CN)_6^{3-/4-}$ (curve a). With the modification of the electrochemically reduced graphene on GCE (GNs/GCE), the semicircles decrease distinctively, indicating that the presence of GNs has accelerated electron transfer between the electrochemical probe of $[Fe(CN)_6]^{3-/4-}$ and the electrode (curve b). With the further coating of QDs onto GNs/GCE (labeled as QDs–GNs/GCE), the semicircle increases significantly as compared to GNs/GCE, suggesting the

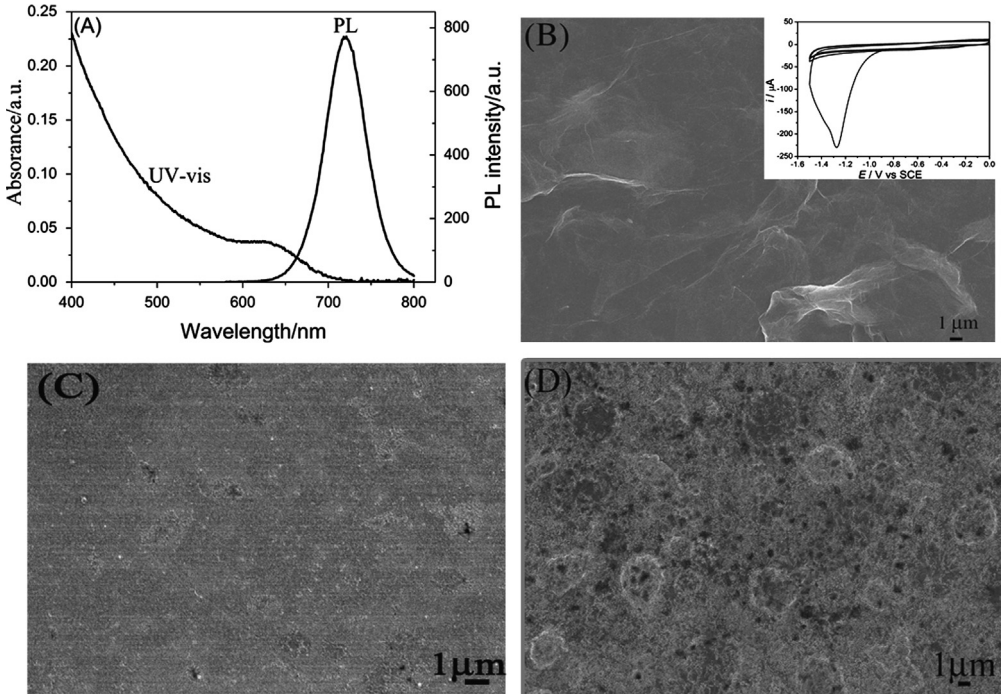

Fig. 1. (A) PL and UV–vis absorption spectra of the CdTe QDs in aqueous solution. Representative SEM images of (B) GNs/GCE, (C) QDs–GNs/GCE, and (D) AChE–QDs–GNs/GCE.

hindrance effect of the semiconductor QDs to the interfacial charge transfer (curve d). After the immobilization of AChE onto QDs–GNs/GCE, the semicircles further increased distinctively (curve e). Obviously, the nonconductive properties of proteins would obstruct electron transfer and mass transport of the electrochemical probe, resulting in the increased resistance. Compared with the intrinsic QDs modified GCE (curve c), the semicircle decreases significantly whether for QDs–GNs/GCE or AChE–QDs–GNs/GCE, further confirming that the presence of GNs facilitated the electron transfer.

3.2. Electrochemiluminescence behavior

ECL signals at each immobilization steps were recorded to monitor the fabrication of the ECL biosensors (Fig. 2B). In air-saturated PBS, the ECL emission of QDs–GNs/GCE could be greatly improved as compared with intrinsic QDs modified GCE. The ECL peak intensity of QDs–GNs/GCE at – 2.48 V was 9566 (Fig. 2B, curve c), while the peak intensity of QDs/GCE was 291 (curve b), indicating an improvement by 33 times. With AChE conjugation onto QDs–GNs/GCE, the ECL peak intensity was decreased to 6148 due to a barrier aroused from AChE for electron and mass transfer of ECL reagents towards the electrode surface (curve d). Upon addition of acetylcholine (ATCl), the AChE catalyzed its hydrolysis to produce choline, which was oxidized by dissolved O_2 as coreactant of CdTe QDs ECL. The consumption of coreactant induced the ECL signal decrease (curve e). Since no obvious ECL emission could be observed at bare GCE, GNs and AChE–GNs modified GCE, the ECL emission should be produced from QDs.

Effect of dissolved oxygen on ECL intensity was also investigated in the following experiments. As shown in Fig. 2C, when dissolved O_2 was removed from the solution by bubbling high-purity N_2, the ECL peak intensity of AChE–QDs–GNs/GCE decreased dramatically (curve a), around 872, compared with the value of ~9566 observed in air-saturated solution (curve b). It suggests that the dissolved O_2 was an important coreactant to produce strong ECL. Furthermore, in N_2-saturated PBS, the ECL peak of AChE–QDs–GNs/GCE did not disappear completely, indicating that N_2 atmosphere did not completely eliminate O_2 from the neighborhood area of AChE–QDs–GNs/GCE, together with a strong adsorption of O_2. Obviously, both the high electronic conductivity of GNs and the adsorption ability toward O_2 exerted the great roles for the improved ECL emission of QDs. To acquire stable ECL, air-saturated CdTe QD solution was recommended in our experiments.

The stability and reproducibility of an AChE–QDs–GNs/GCE were studied in ECL system, as shown in Fig. 2D. It was found that the electrode was very stable and had an excellent reproducibility for ECL of AChE–QDs–GNs when the sensors had been used and then stored in the PBS buffer solution for 2 weeks at 4 °C, which could avoid the serious electrode fouling.

3.3. Optimization of reaction conditions

To get high-performance ECL response, we further optimized the experimental parameters, including the concentration of GO dispersion (C_{GO}), the amount of QDs deposited (C_{QDs}), pH of the solution and potential scan rate (ν). The ECL peak intensity enhanced steadily as C_{GO} grew up to 0.15 mM (Fig. 3A), which indicated that the more condensed state of GNs would more efficiently facilitate the generation of the electron-injected QDs. However, the ECL peak intensity decreased dramatically with C_{GO} over 0.15 mM. It has reported that carbon nanomaterials can

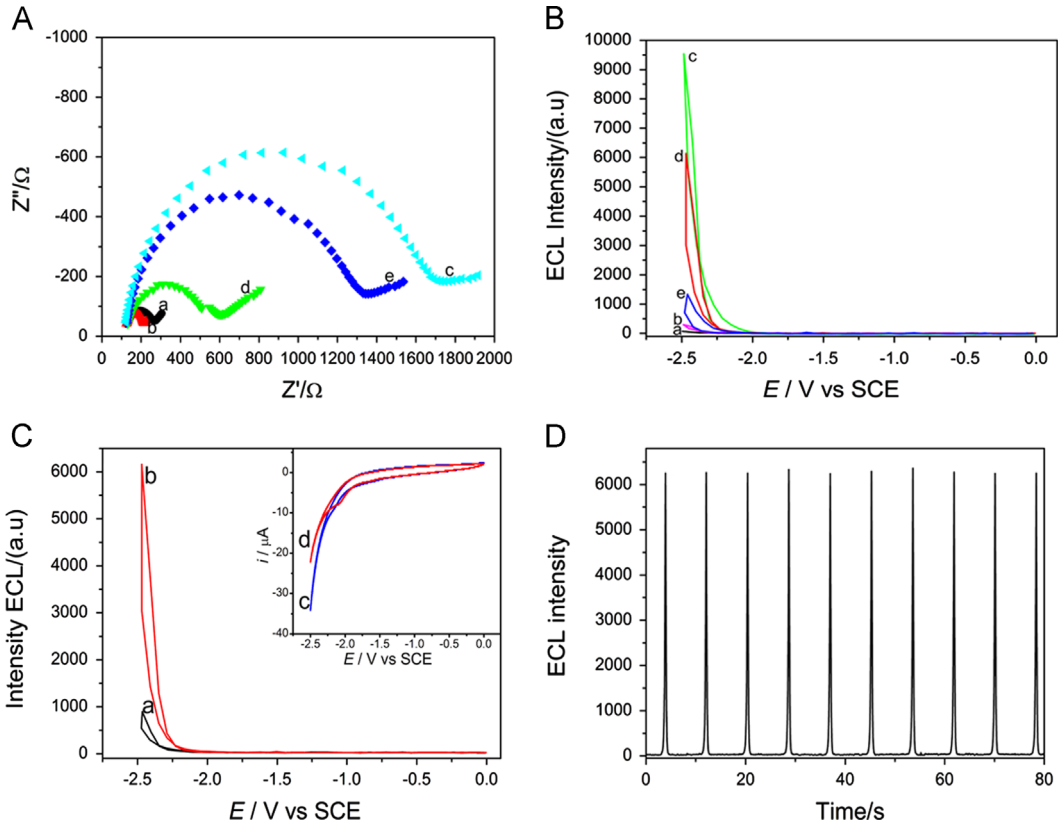

Fig. 2. (A) EIS Nyquist plots of (a) bare GCE, (b) GNs/GCE, (c) QDs/GCE, (d) QDs–GNs/GCE, and (e) AChE–QDs–GNs/GCE in 2.5 mM $[Fe(CN)_6]^{3-/4-}$ +0.1 M KCl. The applied frequency was from 0.01 Hz to 100 kHz. (B) ECL–potential curves of (a) bare GCE, (b) QDs/GCE, (c) QDs–GNs/GCE, (d) AChE–QDs–GNs/GCE in air-saturated 0.1 M pH 8.0 PBS, and (e) AChE–QDs–GNs/GCE in air-saturated 0.1 M pH 8.0 PBS containing 1 mM ATCl; (C) ECL–potential curves of AChE–QDs–GNs/GCE in (a) N_2-saturated, (b) air-saturated 0.1 M pH 8.0 PBS. Inset: the corresponding CV curves in (c) N_2-saturated, and (d) in air-saturated 0.1 M PBS; (D) ECL responses of AChE–QDs–GNs/GCE in air-saturated 0.1 M pH 8.0 PBS. ECL conditions: the potential window: −2.5 to 0 V; scan rate: 0.6 V/s; PMT voltage, 800 V.

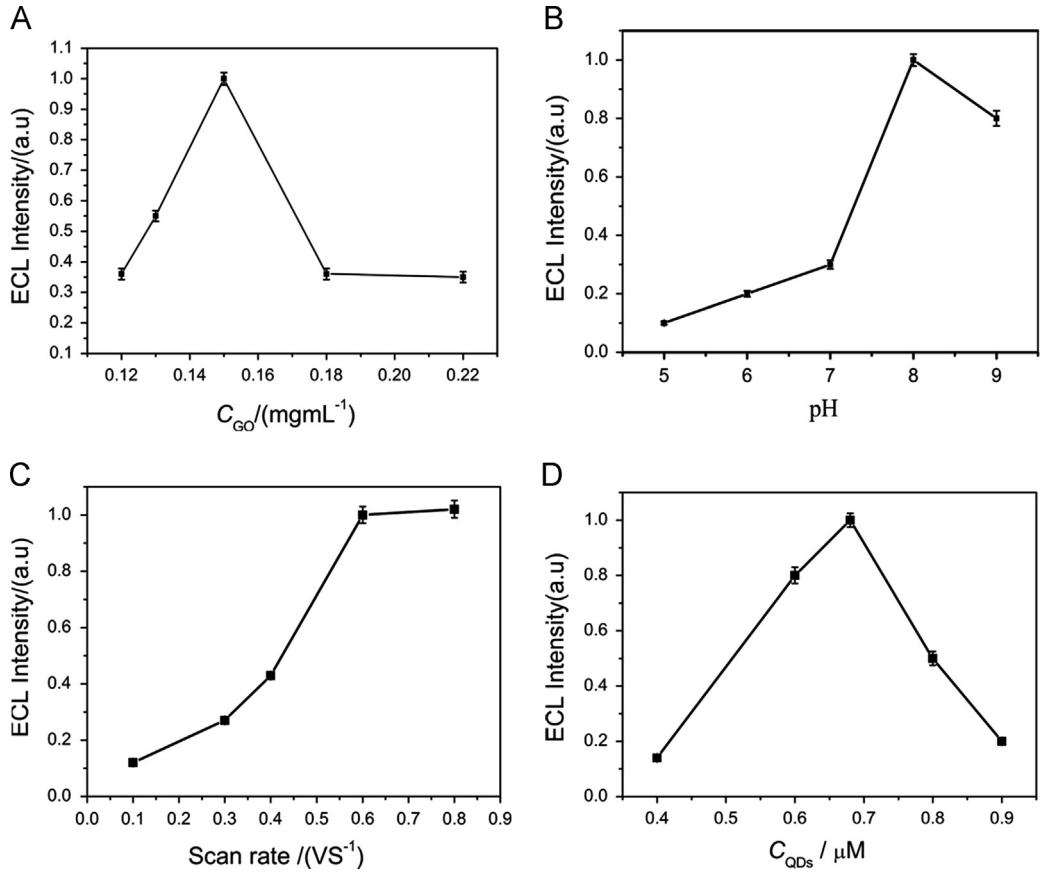

Fig. 3. Effects of (A) the amount of exfoliated GO precasted onto GCE, (B) the solution pH, (C) potential scan rate and (D) the amount of QDs deposited on ECL peak intensity of AChE–QDs–GNs/GCE.

absorb light as a blackbody. Thus C_{GO} for electrochemical reduction was chosen to be 0.15 mM.

The ECL emission of QDs was also dependent on pH of the solution. As shown in Fig. 3B, the ECL intensity increased with pH changing from 5.0 to 8.0. Considering that a much higher pH value over 9.0 was unfavorable for further application, pH 8.0 PBS was used as the detection solution.

The scan rate could affect the ECL over a wide range, since the ECL efficiency significantly depended on the rate of generation/annihilation of R^* (Jiang and Ju, 2007) High scan rate could enrich R^* in a short time span enhancing ECL intensity (Fig. 3C). The ECL intensity increased with the increasing scan rate and kept steady at 600 mV s^{-1}, indicating the emitted photons came to saturation.

The amount of CdTe QDs dispersed onto GNs/GCE sharply influenced the ECL peak intensity, directly related with the quantity of the excited state R^*. With increasing the amount of CdTe QDs onto GNs/GCE, the formed individual nanocrystal species increased during the cathodic scan, leading to the enhancement in ECL intensity. The final ECL peak intensity at QDs–GNs/GCE at first was up to 0.7 μM and then decreased at higher concentration (Fig. 3D). It indicated that the over-loaded QDs increased the film thickness and inhibited the electron exchange with radical species.

The concentration of ATCl was one of the another most influential parameters. When the concentration of ATCl was too low, the enzymatic reaction was so weak that the determination of MP is hardly feasible. However, too high substrate concentration would cause all the active centers of AChE being occupied by the substrate and insensible to the inhibitor. Thus, the concentration of 1.0 mM ATCl is chosen for the subsequent experiment (Fig. S1).

3.4. Analytical performance for methyl parathion using AChE/QDs/ERGO/GCE

Fig. 4 displays the ECL responses of AChE–QDs–GNs/GCE in the presence of different concentrations of methyl parathion (MP). Under the optimal conditions, the ECL peak intensity increased with increasing concentration of MP. Well-defined peaks, proportional to the concentration of the corresponding MP, were observed in two ranges, from 0.2 ng mL^{-1} to 10 ng mL^{-1} and 20 ng mL^{-1} to 150 ng mL^{-1}. The linearization equations were *ECL intensity* = 3154.25 + 117.40 c/ng mL^{-1} and *ECL* intensity = 4690.02 + 9.34 c/ng mL^{-1}, with the correlation coefficients of R = 0.9967 and R = 0.9966, respectively (inset of Fig. 4). A detection limit of 0.06 ng mL^{-1} was obtained with the calculation based on signal-noise ratio equal to 3. It is significantly lower than 13.2 ng mL^{-1} at a carbon-paste electrode (Liu and Lin, 2005), lower than those using enzyme-based electrochemical sensors (Gong et al., 2009, 2012a, 2013; Liu and Lin, 2005; Kok and Hasirci, 2004; Wang et al., 2010), also lower than those with 1.0 ng mL^{-1} at ZrO_2NPs, LDHs-based SPE (Gong et al., 2012b; Liang et al., 2012b), and comparable with that reported using photoelectrochemical sensor (Gong et al., 2012a). The stability of the AChE–QDs–GNs modified electrode could be maintained by being stored at 4 °C in a dry condition. No obvious decrease in the response of MP was observed in the first 10-day storage. After a 30-day storage period, the sensor retained 92% of its initial current response. A series of 5 repetitive determinations of 10 ng mL^{-1} MP yielded reproducible ECL peak intensity with relative standard deviations of 3.2%.

The interferences from the other electroactive nitrophenyl derivatives, such as trinitrotoluene (TNT), nitrobenzene, p-nitrophenol,

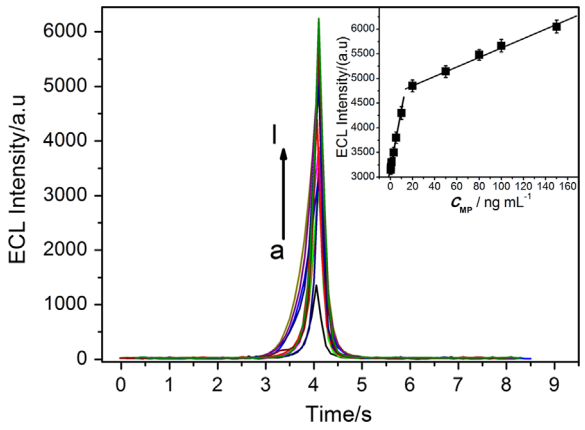

Fig. 4. ECL–time curves of the AChE–QDs–GNs/GCE in the absence (a) and presence (b–i) of different concentrations of MP: (a) 0, (b) 0.2, (c) 0.6, (d) 1, (e) 3, (f) 5, (g) 10, (h) 20, (i) 50, (j) 80, (k) 100, and (l) 150 ng mL^{-1}. The inset shows calibration curve for MP determination. Error bars indicate the standard deviations ranging from 2.1% to 3.0% (n=3). ECL conditions: scan rate: 0.6 V/s; PMT voltage, 800 V.

Table 1
ECL detection of methyl parathion in real samples using the proposed method (n=5).

Sample	Concentration		RSD (%)	Recovery (%)
	Taken (ng mL^{-1})	Found (ng mL^{-1})		
Cabbage 1	0.00	0.00	_	
Cabbage 2	10.00	9.45	0.41	94.5
Cabbage 3	40.00	41.02	1.20	102.6
Cabbage 4	100.00	98.33	1.10	98.3

and other oxygen-containing inorganic ions (PO_4^{3-}, SO_4^{2-}, NO_3^-) (listed in Supplementary data as Fig. S2). No obvious inhibition behavior can be observed with the ECL intensity varied slightly.

The AChE inhibited irreversibly by OPs could be reactivated by use of nucleophilic compounds such as pralidoxime iodide. It was observed that AChE modified electrode inhibited by methyl parathion could resume 91% original activity after immersing in 7.0 mM pralidoxime iodide (Fig. S3a). With increasing reactivation time, the reactivation efficiency *R*% increased and reached stable at ~20 min (Fig. S3b). Based on this reactivation procedure, the proposed biosensor could be used repeatedly with an acceptable reproducibility.

To further demonstrate the practicality of the present electrode, it was evaluated by processing real samples. We performed the recovery tests by adding different amounts of MP into real samples, including cabbage, summarized as Table 1. The recoveries of the spiked MP are from 94.5% to 102.6% for the real samples, indicating that the proposed method can be used for direct analysis of relevant samples with high accuracy and reproducibility.

4. Conclusions

In summary, a novel signal-on ECL biosensor has been developed for the determination of methyl parathion, where the smart integration of electrochemically reduced graphene (ERG), QDs and biomolecules AChE yields a biofunctional AChE–ERG–CdTe QDs hybrid as cathodic ECL emitters for OPs sensing. Based on the consumption of dissolved O_2 in enzymatic reaction, a highly sensitive signal-on ECL biosensor has been constructed. The resulting biosensor showed good sensitivity, reproducibility, ideal stability and fine applicability for the detection of methyl parathion in real samples. We believe that the combination of graphene, enzyme reaction, the dissolved oxygen as coreactant, and QDs-based ECL opens up new opportunities for fast, simple and sensitive analysis of OPs.

Acknowledgments

This work was supported by National Science Foundation of China (Grant 20803026, 21175053), the Program for Chenguang Young Scientist for Wuhan (201271031412), the Program for Distinguished Young Scientist of Hubei Province (2013CFA030), and the Program for New Century Excellent Talents in University of China (NCET-13-0815).

Appendix A. Supporting information

Supplementary data associated with this article can be found in the online version at http://dx.doi.org/10.1016/j.bios.2013.10.011.

References

Albanis, T.A., Hela, D.G., Lambropoulou, D.A., Sakkas, V.A., 2004. Int. J. Environ. Anal. Chem. 84, 1079–1092.
Arduini, F., Ricci, F., Tuta, C.S., Moscone, D., Amine, A., Palleschi, G., 2006. Anal. Chim. Acta 580, 155–162.
Bachmann, R.W., Hoyer, M.V., Canfield Jr., D.E., 1999. Hydrobiologia 394, 219–232.
Bertolino, C., MacSweeney, M., Tobin, J., O'Neill, B., Sheehan, M.M., Coluccia, S, Berney, H., 2005. Biosens. Bioelectron. 21, 565–573.
Chauhan, N., Pundir, C.S., 2012. Electrochim. Acta 67, 79–86.
Cheng, C.M., Huang, Y., Tian, X.Q., Zheng, B.Z., Li, Y., Yuan, H.Y., Xiao, D., Xie, S.P., Choi, M.M.F., 2012. Anal. Chem. 84, 4754–4759.
Dai, H., Wang, Y.M., Wu, X.P., Zhang, L., Chen, G.N., 2009. Biosens. Bioelectron. 24, 1230–1234.
Deng, S.Y., Lei, J.P., Cheng, L.X., Zhang, Y.Y., Ju, H.X., 2011. Biosens. Bioelectron. 26, 4552–4558.
Dennany, L., Forster, R.J., Rusling, J.F., 2003. J. Am. Chem. Soc. 125, 5213–5218.
Ding, Z.F., Quinn, B.M., Haram, S.K., Pell, L.E., Korgel, B.A., Bard, A.J., 2002. Science 296, 1293–1297.
Ding, S.N., Xu, J.J., Chen, H.Y., 2006. Chem. Commun., 3631–3633.
Gong, J.M., Miao, X.J., Wan, H.F., Song, D.D., 2012b. Sens. Actuat. B 162, 341–347.
Gong, J.M., Guan, Z.Q., Song, D.D., 2013. Biosens. Bioelectron. 39, 320–323.
Gong, J.M., Wang, L.Y., Song, D.D., Zhu, X.L., Zhang, L.Z., 2009. Biosens. Bioelectron. 25, 493–496.
Gong, J.M., Wang, X.Q., Li, X., Wang, K.W., 2012a. Biosens. Bioelectron. 38, 43–49.
Guo, H.L., Wang, X.F., Qian, Q.Y., Wang, F.B., Xia, X.H., 2009. ACS Nano 3, 2653–2659.
Guo, Z.H., Dong, S.J., 2004. Anal. Chem. 76, 2683–2688.
Han, E., Ding, L., Lian, H.Z., Ju, H.X., 2010. Chem. Commun. 46, 5446–5448.
Huang, H.P., Zhu, J.J., 2009. Biosens. Bioelectron. 25, 927–930.
Huang, H.P., Li, J.J., Tan, Y.L., Zhou, J.J., Zhu, J.J., 2010. Analyst 135, 1773–1778.
Huang, H.P., Li, J.J., Zhu, J.J., 2011. Anal. Methods 3, 33–42.
Hummers, W., Offeman, J., 1958. J. Am. Chem. Soc. 80, 1339.
Jiang, H., Ju, H.X., 2007. Anal. Chem. 79, 6690–6696.
Jie, G.F., Yuan, J.X., 2012. Anal. Chem. 84, 2811–2817.
Kim, T.H., Kuca, K., Jun, D., Jung, Y.K., 2005. Bioorg. Med. Chem. Lett. 15, 2914–2917.
Kok, F.N., Hasirci, V., 2004. Biosens. Bioelectron. 19, 661–665.
Kovtyukhova, N.I., Ollivier, P.J., Martin, B.R., Mallouk, T.E., Chizhid, S.A., Buzaneva, E.V., Gorchinskiy, A.D., 1999. Chem. Mater. 11, 771–778.
Kurita, R., Arai, K., Nakamoto, K., Kato, D., Niwa, O., 2010. Anal. Chem. 82, 1692–1697.
Leandro, C.C., Hancock, P., Fussell, R.J., Keely, B.J., 2006. J. Chromatogr. A 1103, 94–101.
Lei, J.P., Ju, H.X., 2011. Trends Anal. Chem. 30, 1351–1359.
Li, B.X., He, Y.Z., Xu, C.L., 2007. Talanta 72, 223–230.
Li, J., Guo, S.J., Wang, E.K., 2012. RSC Adv. 2, 3579–3586.
Li, J.H., Zhou, J.J., Han, H.Y., 2010. Electrochim. Acta 55, 1265–1271.
Li, L.L., Chen, Y., Lu, Q., Ji, J., Shen, Y.Y., Xu, M., Fei, R., Yang, G.H., Zhang, K., Zhang, J.R., Zhu, J.J., 2013. Sci. Rep., 3, http://dx.doi.org/10.1038/srep015291529.
Li, L.L., Liu, K.P., Yang, G.H., Wang, C.M., Zhang, J.R., Zhu, J.J., 2011. Adv. Funct. Mater. 21, 869–878.
Liang, G.D., Liu, S.F., Zou, G.Z., Zhang, X.L., 2012a. Anal. Chem. 84, 10645–10649.
Liang, H., Miao, X.J., Gong, J.M., 2012b. Electrochem. Commun. 20, 149–152.
Liao, S.Z., Han, W.T., Ding, H.Z., Xie, D.X., Tan, H., Yang, S.Y., Wu, Z.Y., Shen, G.L., Yu, R.Q., 2013. Anal. Chem. 85, 4968–4973.
Liu, G.D., Lin, Y.H., 2005. Electrochem. Commun. 7, 339–343.
Liu, X., Jiang, H., Lei, J.P., Ju, H.X., 2007. Anal. Chem. 79, 8055–8060.
Liu, X., Ju, H.X., 2008. Anal. Chem. 80, 5377–5382.
Liu, X., Zhang, Y.Y., Lei, J.P., Xue, Y.D., Cheng, L.X., Ju, H.X., 2010. Anal. Chem. 82, 7351–7356.

Liu, W.Y., Zhang, Y., Ge, S.G., Song, X.R., Huang, J.D., Yan, M., Yu, J.H., 2013. Anal. Chim. Acta 770, 132–139.
Miao, W., 2008. Chem. Rev. 108, 2506–2553.
Nie, G.M., Bai, Z.M., Yu, W.Y., Chen, J., 2013. Biomacromolecules 14, 834–840.
Qiu, S.Y., Gao, S., Zhu, X., Lin, Z.Y., Qiu, B., Chen, G.N., 2011. Analyst 136, 1580–1585.
Rampazzo, E., Bonacchi, S., Genovese, D., Juris, R., Marcaccio, M., Montalti, M., Paolucci, F., Sgarzi, M., Valenti, G., Zaccheroni, N., Prodi, L., 2012. Coord. Chem. Rev. 256, 1664–1681.
Richter, M.M., 2004. Chem. Rev. 104, 3003–3036.
Rotiroti, L., Stefano, L.D., Rendina, I., Moretti, L., 2005. Biosens. Bioelectron. 20, 2136–2139.
Shan, Y., Xu, J.J., Chen, H.Y., 2009. Chem. Commun. 8, 905–907.
Shen, Z.L., Nakayama, S.Z., Semancik, S., Sintim, H.O., 2012. Chem. Commun. 48, 7580–7582.
Wang, J., Han, H.Y., Jiang, X.C., Huang, L., Chen, L.N., Li, N., 2012. Anal. Chem. 84, 4893–4899.
Wang, X.Y., Yun, W., Dong, P., Zhou, J.M., He, P.G., Fang, Y.Z., 2008. Langmuir 24, 2200–2205.
Wang, X.F., Zhou, Y., Xu, J.J., Chen, H.Y., 2009a. Adv. Funct. Mater. 19, 1–7.
Wang, Y., Lu, J., Tang, L.H., Chang, H.X., Li, J.H., 2009b. Anal. Chem. 81, 9710–9715.
Wang, Y.Z., Qiu, H.X., Hu, S.Q., Xu, J.H., 2010. Sens. Actuat. B 147, 587–592.
Won, Y.-H., Jang, H.S., Kim, S.M., Stach, E., Ganesana, M., Andreescu, S., Stanciu, L.A., 2010. Langmuir 26, 4320–4326.
Yang, S.L., Liang, J.S., Luo, S.L., Liu, C.B., Tang, Y.H., 2013. Anal. Chem. 85, 7720–7725.
Yu, W.W., Qu, L.H., Guo, W.Z., Peng, X.G., 2003. Chem. Mater. 15, 2854–2860.
Zhang, J., Qi, H.L., Li, Y., Yang, J., Gao, Q., Zhang, C.X., 2008. Anal. Chem. 80, 2888–2894.
Zhang, Y.Y., Deng, S.Y., Lei, J.P., Xu, Q.N., Ju, H.X., 2011. Talanta 85, 2154–2158.